NASA-TM-106751
19950007137

NASA Technical Memorandum 106751
ICOMP–94–23; AIAA–94–0835

Numerical Simulations of Drop Collisions

M.R.H. Nobari
University of Michigan
Ann Arbor, Michigan

and

G. Tryggvason
Institute for Computational Mechanics in Propulsion
Lewis Research Center
Cleveland, Ohio

and University of Michigan
Ann Arbor, Michigan

Prepared for the
32nd Aerospace Sciences Meeting and Exhibit
sponsored by the American Institute of Aeronautics and Astronautics
Reno, Nevada, January 10–13, 1994

National Aeronautics and
Space Administration

NUMERICAL SIMULATIONS OF DROP COLLISIONS

M.R.H. Nobari*
The University of Michigan
Ann Arbor, MI
and
G. Tryggvason†
Institute for Computational Mechanics in Propulsion,
Lewis Research Center, Cleveland, OH
and
The University of Michigan
Ann Arbor, MI

Abstract

Three-dimensional simulations of the off-axis collisions of two drops are presented. The full Navier-Stokes equations are solved by a Front-Tracking/Finite-Difference method that allows a fully deformable fluid interface and the inclusion of surface tension. The drops are accelerated towards each other by a body force that is turned off before the drops collide. Depending on whether the interface between the drops is ruptured or not, the drops either bounce or coalesce. For drops that coalesce, the impact parameter, which measures how far the drops are off the symmetry line, determines the eventual outcome of the collision. For low impact parameters, the drops coalesce permanently, but for higher impact parameters, a grazing collision, where the drops coalesce and then stretch apart again is observed. The results are in agreement with experimental observations.

Introduction

The dynamic of fluid drops is of considerable importance in a number of engineering applications and natural processes. The combustion of fuel sprays, spray painting, various coating processes, as well as rain, are only a few of the more common examples. While it is usually the collective behavior of many drops that is of interest, often it is the motion of individual drops that determines the large scale properties of the system. Thus, for example, the total surface area of sprays depends on the size of the individual drops as well as their number density. Computational models for engineering predictions of spray combustion generally do not resolve the motion of individual drops and must rely on "subgrid" models where the average effects of the unresolved scales are incorporated into the equations used to predict the large scale behavior. Many spray models (see Heywood[1], for a discussion and references) use point particles to represent the drops. The drop motion is related to the fluid flow by empirical laws for drag, heat transfer and combustion. Often it is possible to focus on the dynamic of a single drop and how it interacts with the surrounding flow. When the number of drops per unit volume is high, however, it is necessary to account for the interactions between the drops and their collective effect on the flow. To account for drop collisions, models must contain "collision rules" that determine whether the drops coalesce or not. These rules are usually based on experimental investigations of binary collisions of drops, but the small spatial and temporal scales make detailed experimental measurements difficult and usually the record consist of little more than photographs or a video tape. Since the collision process generally involves large drop deformation and rupture of the interface separating the drops, it has not been amenable to detailed theoretical analysis. Previous studies are therefore mostly experimental, but sometimes supplemented by greatly simplified theoretical argument.

Two recent experimental investigations of drop collisions can be found in Azhgriz and Poo[2], and Jiang, Umemura and Law[3] who show several photographs of the various collision modes for both water and hydrocarbon drops. These, and other experimental investigations have provided considerable information and, in particular, it is now understood that the outcome of a collision can be classified into about five main categories. For head-on collisions we have four main categories: bouncing collision, where the drops collide and separate, retaining their identity; coalescence collision, where two drops become one; separation collision, where the drops temporarily become one but then break up again; and shattering collision, where the impact is so strong that the drops break up into several smaller drops. These categories survive for off-axis collisions, but a fifth one,

*Graduate Student, Department of Mechanical Engineering

†Associate Professor, Department of Mechanical Engineering

grazing or stretching collision, appears. Here, the drops coalesce upon contact, but are sufficiently far apart so that they continue along the original path and separate again. The form of the collision depends on the size of the drops, their relative velocities, their off-axis position and the physical properties of the fluids involved. For a given fluid, some of these collision regimes are not observer. Water drops, for example, do not show bouncing. (Jiang *et al.*[3], state that they also did not find reflective collision for water drops. This is apparently due to a limited parameter range studied by them as the experiments by Azhgriz and Poo[2], show.) Other investigations of drop collisions may be found in Bradley and Stow[4], and Podvysotsky and Shraiber[5], for example. The major goal of these investigations has been to clarify the boundaries between the major collision categories and explain how they depend on the parameters of the problem. Simple models used to rationalize experimental findings have been presented by Park and Blair[6], Ryley and Bennett-Cowell[7], Brazier-Smith et al.[8], Azhgriz and Poo[2], and Jiang, Umemura and Law[3].

In principle, numerical solutions of the Navier-Strokes equations, where all scales of motion are fully resolved, can provide the missing information, but various numerical difficulties associated with moving boundaries between two fluids have made detailed simulations difficult in the past. Nevertheless, several authors have computed the axisymmetric head-on collision of drops with a wall. The earliest work is Foote[9] who followed the evolution of a rebounding axisymmetric drops at low Weber number using the MAC method. More recent computations work can be found in Fukai et al[10] who use a moving finite element method. We have recently conducted a numerical study of the head-on collision of two axisymmetric drops, see Nobari, Jan and Tryggvason[11], where we examined the boundary between coalescing and reflecting collision for equal size drops. Here, we present numerical simulations of three-dimensional, off-axis collisions, where the full Navier Stokes equations are solved to give a detailed picture of the flow during collision.

Formulation and Numerical Method

The numerical technique used for the simulations presented in this paper is the Front Tracking/Finite Difference method of Unverdi and Tryggvason[12, 13]. Since the procedure has bee described in detail before, we only outline it briefly here.

The physical problem and the computational domain is sketched in Figure 1. The domain is a rectangular box and the drops are initially placed near each end of the domain. A force that is turned off before the drops collide, is applied to drive them together initially. Generally, the density and viscosity of the ambient fluid are much smaller than of the drop fluid and thus have only a small effect on the results. While it is therefore often sufficient to solve only for the fluid motion inside the drop, here we solve for the motion everywhere, both inside and outside the drops. The Navier-Stokes equations are valid for both fluids, and a single set of equations can be written for the whole domain as long as the jump in viscosity and density is correctly accounted for and surface tension is included:

$$\frac{\partial \rho \bar{u}}{\partial t} + \nabla \cdot \rho \bar{u}\bar{u} = -\nabla p + \bar{f}_x + \nabla \cdot \mu\left(\nabla \bar{u} + \nabla \bar{u}^T\right) + \bar{F}_\sigma \delta\left(\bar{x} - \bar{x}_f\right).$$

Here, $\bar{u}$ is the velocity, p is the pressure, and ρ and μ are the discontinuous density and viscosity fields, respectively. $\bar{F}_\sigma$ is the surface tension force and $\bar{f}_x$ is a body force used to give the drops their initial velocity. Notice that the surface tension force has been added as a delta function, only affecting the equations where the interface is. The detailed form of $\bar{F}_\sigma$ will be discussed below. The above equations are supplemented by the incompressibility conditions

$$\nabla \cdot \bar{u} = 0$$

which, when combined with the momentum equations leads to a non-separable elliptic equation for the pressure. We also have equations of state for the density and viscosity:

$$\frac{\partial \rho}{\partial t} + \bar{u} \cdot \nabla \rho = 0$$

$$\frac{\partial \mu}{\partial t} + \bar{u} \cdot \nabla \mu = 0.$$

These last two equations simply state that density and viscosity within each fluid remains constant.

Nondimensionalization gives a Weber and a Reynolds number defined by:

$$We = \frac{\rho_d D U^2}{\sigma}; \quad Re = \frac{\rho_d U D}{\mu_d}$$

In addition, the density ratio $r = \rho_d / \rho_o$ and the viscosity ratio $\lambda = \mu_d / \mu_o$ must be specified. Here, the subscript d denotes the drop fluid and o the ambient fluid. In off-axis collisions, the drops approach each other along parallel lines that are some distance apart. If this distance is greater than the drop diameter, D, the drops never touch and no collision takes place. If this distance is zero, we have a head-on collision. To describe off-centered

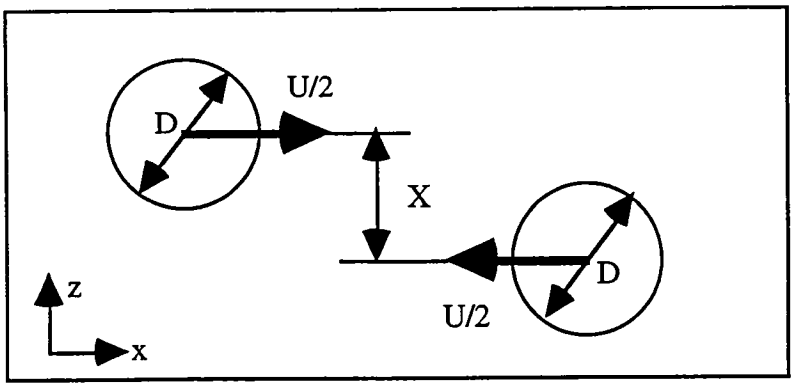

Figure 1. The computational domain and the initial conditions. The drops are initially two and a half diameter apart.

collision a new nondimensional parameter, usually called the impact parameter, is required in addition to the Weber and the Reynolds number defined earlier. This parameter is usually defined as

$$I = \frac{\chi}{D}$$

where χ is the perpendicular distance between the lines that the drops move along before collision.

The force used to drive the drops together initially is taken as

$$\bar{f}_x = C(\rho - \rho_o)(x - x_c)$$

so the force acts only on the drops. Here C is an adjustable constant and x_c is midway between the drops. This force is turned off before the actual collision takes place. Initially, the drops are place with their centers two and a half diameter between them, and C is varied to give different collision velocities.

To solve the Navier Stokes equations we use a fixed, regular, staggered grid and discretize the momentum equations using a conservative, second order centered difference scheme for the spatial variables and an explicit second order time integration method. The pressure equation, which is non-separable due to the difference in density between the drops and the ambient fluid, is solved by a Black and Red SOR scheme. Other versions of our code use a multigrid iteration. The novelty of the scheme is the way the boundary, or the front, between the drops and the ambient fluid is tracked. The front is represented by separate computational points that are moved by interpolating their velocity from the grid. These points are connected by triangular elements to form a front that is used to keep the density and viscosity stratification sharp and to calculate surface tension forces. At each time step information must be passed between the front and the stationary grid. This is done by a method similar to the one discussed by Unverdi and Tryggvason[12], that spreads the density jump to the grid points next to the front and generates a smooth density field that changes from one density to the other over two to three grid spaces. While this replaces the sharp interface by a slightly smoother grid interface, all numerical diffusion is eliminated since the grid-field is reconstructed at each step. The surface tension forces are computed from the geometry of the interface and distributed to the grid in the same manner as the density jump. Generally, curvature is very sensitive to minor irregularity in the interface shape and it is difficult to achieve accuracy and robustness at the same time. However, by computing the surface tension forces directly by

$$\bar{F}_\sigma = \sigma \oint \bar{t} \times \bar{n} ds$$

we ensure that the net surface tension force is zero, or:

$$\oint \sigma \kappa \bar{n} ds = 0$$

Here, $\bar{n}$ is the outward normal, $\bar{t}$ a tangent vector to the boundary curve for each element and κ is twice the mean curvature. This is important for long time simulations since even small errors can lead to a net force that moves the drop in an unphysical way.

As the drops move and deform, it is necessary to add and delete points at the front and to modify the connectivity of the points, to keep the front elements of approximately equal size and as "well shaped" as possible. This is described in Unverdi and Tryggvason.[12] When the drops are close, we rupture the interface, in several of our computations, by removing surface elements that are nearly parallel and reconnecting the remaining ones to form a single surface. Here, this restructuring of the interface is done at prescribed time if the interfaces are close enough. While this rather arbitrary (and we have simply selected the

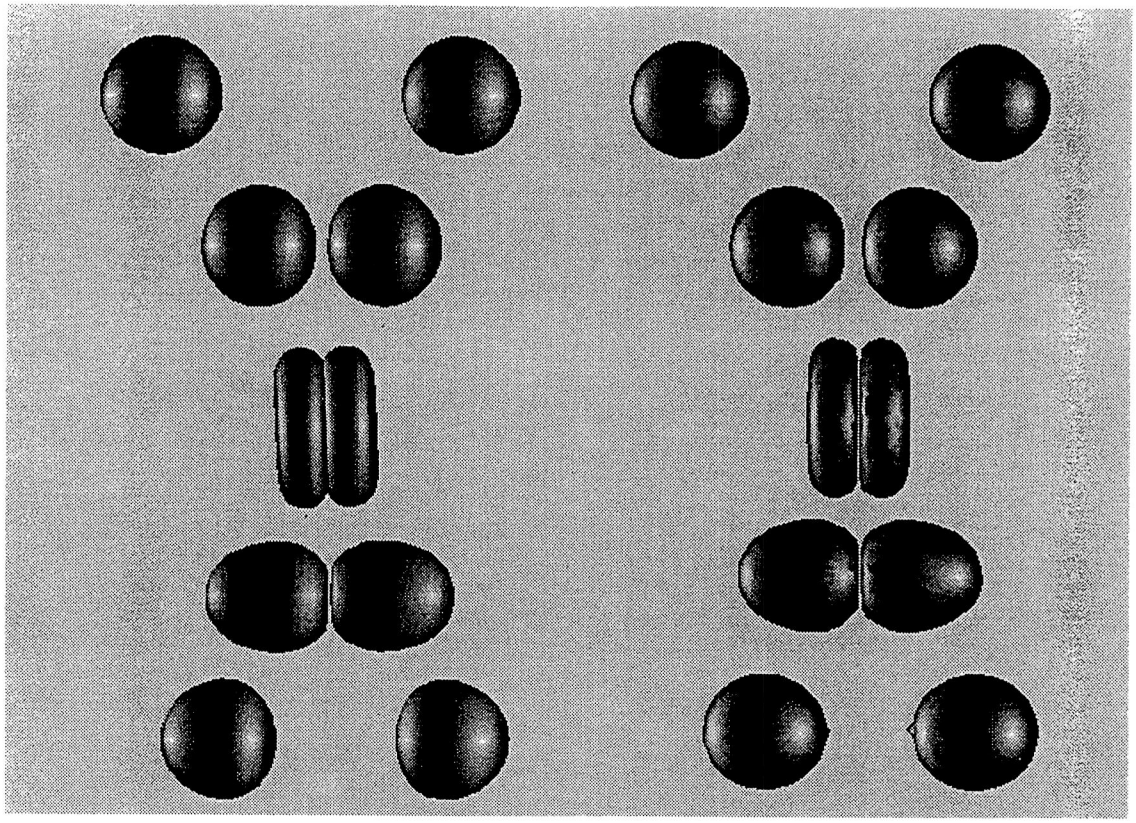

Figure 2. Comparison between a fully three-dimensional simulation (right) and results obtained by an axisymmetric code (left). The initial conditions are shown at the top of each column and the solution is then shown at three equispaced times for each run.

restructuring of the interface is done at prescribed time if the interfaces are close enough. While this rather arbitrary (and we have simply selected the time when the drops look close enough) this allows some control over the dynamic of the rupture, as compared with numerical methods where the front is not tracked and the film would always rupture once it is thinner than a few grid spaces. For a more detailed discussion of this point see Nobari, Jan, and Tryggvason[4].

The method and the code has been tested in various ways, such as by extensive grid refinement studies, comparison with other published work and analytical solutions. It has also been used to investigate a number of other multifluid problems. In addition to the computations of head-on collisions of drops by Nobari, Jan and Tryggvason[4], Unverdi and Tryggvason[13] simulated the collision of fully three dimensional bubbles, Ervin[14] investigated the lift of deformable bubbles rising in a shear flow (see also Esmaeeli, Ervin, and Tryggvason[15], Jan and Tryggvason[16] examined the effect of contaminants on the rise of buoyant bubbles and Nobari and Tryggvason[17] followed the coalescence of drops of different sizes. Nas and Tryggvason[18] presented simulation of thermal migration of many two dimensional bubbles.

Results and Discussions

For the computations presented here, We=23, Re=68, r=40, and λ=20, but the impact parameter, I, is varied. The computational domain is resolved by a 32 by 32 by 64 cubic mesh and the drop diameter is 0.4 times the shorter dimension.

While we have done extensive checks of the accuracy of our axisymmetric code, the three-dimensional code has not been tested as thoroughly. We have therefore conducted a few calculations of head-on collisions where the results from the three-dimensional simulations can be compared with the axisymmetric results. Figure 2 shows this comparison. The axisymmetric results are to the left and the fully three dimensional results to the right. The initial conditions are shown at the top of each column and the drops are then shown below at equispaced times. The force that acts on the drops initially is turned off before impact (just before the second frame). As the drops collide they become

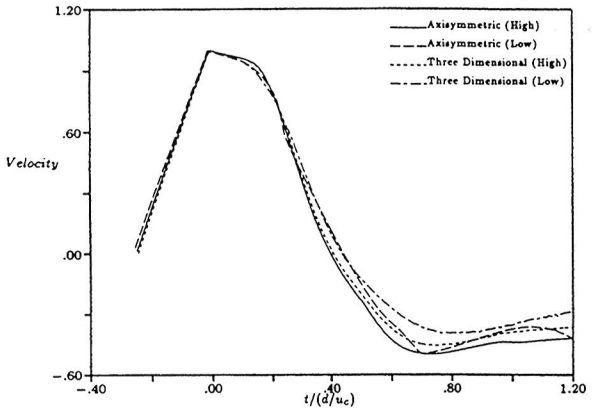

Figure 3. The x-position of the center of mass of one drop versus time, as computed by both the fully three-dimensional code and an axisymmetric one, for two different resolutions.

flatter, and the ambient fluid between them is pushed away, leaving a thin film of fluid between the drops. Here, this film is not removed and the drops therefore rebound, recovering their spherical shape. Obviously, the results are in good agreement. Figure 3 shows a more quantitative comparison, where we plot the x-position of the center of mass for the drops in figure 2, as well as for drops computed on a coarser grid (16 by 16 by 32). The agreement is reasonably good, although the coarse grid results are not in as good agreement with each other as the finer grid results are.

In figure 4, the off-axis collision of two drops, for I=0.75, is shown. The pair is shown at several equispaced times, beginning with the initial position at the top of the figure. Once the drops have the desired velocity, around the third frame from the top, the force that is applied to drive the drops together is turned off. The drops continue to move together, and in the fourth frame they have collided, deforming as they do so. Since the collision parameter is relatively high, the drops slide past each other and continue along their original path. The bottom four frames show the motion of the drops after the collision. During the collision the drops become nearly flat where they face each other, and as the drops slide past each other the fluid layer between the drops becomes progressively thinner. If it becomes thin enough it should rupture, but here we have not allowed that to happen. (As seen in figure 6, rupture of this film will change the resulting evolution considerably.) In figure 5, the velocity components of the center of mass of one of the drops, (a), and the kinetic and the surface tension energy, (b), is plotted versus time. The solid curve in (a) is the velocity in the horizontal direction. It increases as the force accelerates the drops together, and then decreases slightly due to the drag from the outer fluid after

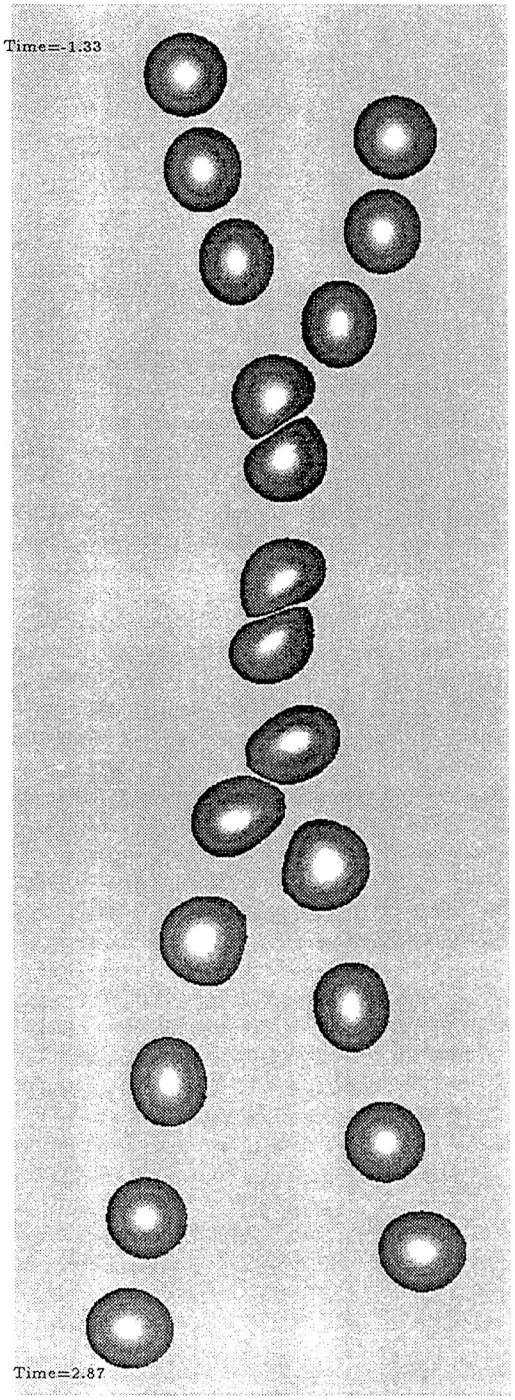

Figure 4. Bouncing collision. Here I=0.75 and the drops are not allowed to coalesce. The initial conditions are shown at the top and the drops are then shown every 0.42 time unit.

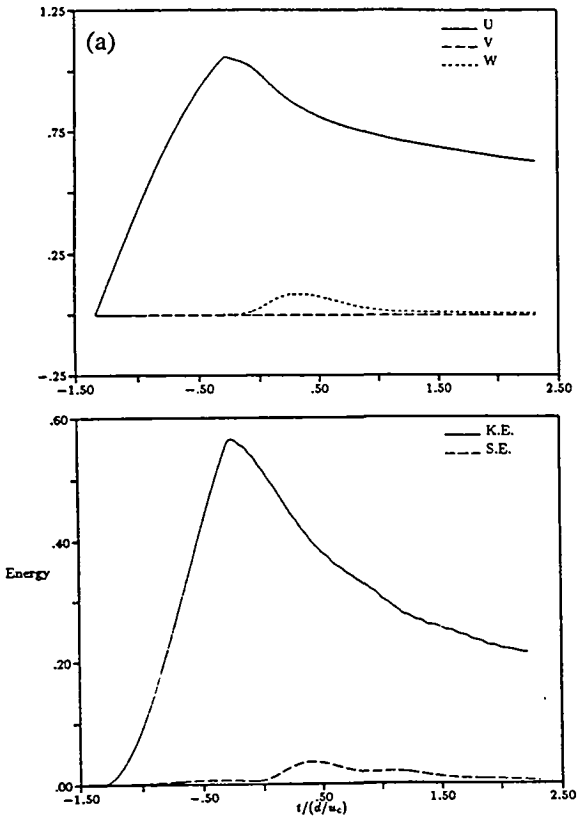

Figure 5. (a) Center of mass velocity of one drop from the computation in figure 4. (b) Kinetic and surface tension energy of one drop.

the force is turned off. When the drops actually collide, it is reduced more rapidly, but eventually resumes a nearly constant decay rate after the collision is over. The velocity component in the vertical direction (short dashes) is non zero only during the actual collision. The kinetic energy in (b) shows similar behavior as the velocity: it decreases slowly after the force is turned off, more rapidly during collision and then resumes slow decay. The surface tension energy rises during the collision as the drop deforms, thus contributing to the reduction in the kinetic energy. Notice that the drop oscillates slightly after the collision as seen in the surface tension energy plot.

Although bouncing is observed for real drops, it is actually a relatively rare outcome of a collision, only seen when the drop deform and trap fluid between them and the velocity is sufficiently large so the film does not have time to drain before the drops rebound. To investigate the behavior of drops that coalesce, we have written software to automatically remove the front bounding the thin film between the drops at a prescribed time and allow the drops to coalesce. Figure 6 shows the results of two computations where the drops coalesce. All parameters are the same as in figure 2, except that in the left column I=0.50, and in the right column I=0.825. The film between the drops is ruptured at time 0.46 for both runs. In these computations we put t=0.0 when the distance between the center of the drops is one diameter. For the low impact parameter case, the drops deform considerably during the initial impact, as observed for head-on collisions, but the impact parameter is sufficiently large so the drops still slide past each other. As the film is ruptured and the drops coalesce the momentum of each drop is sufficiently large so the large combined drop continues to elongate. Eventually, however, surface tension overcomes the stretching and the drop is pulled into a spherical shape. Due to the velocity of the drops that coalesced, the combined drop rotates.

While the low impact parameter drops are in many way similar to drops undergoing a head-on collision, the high impact parameter drops in figure 6b deform only slightly as they collide. When the interface between them is ruptured, they have nearly passed each other and after rupture their momentum is sufficiently large so they continue along their original path and stretch the fluid column connecting them until it is near breaking. We have not written the software necessary for rupturing the filament connecting the drops and therefor must stop the computations at this point. Notice, that the coalesced drop rotates, as the low impact parameter one did, although much less.

In figure 7, the surface tension energy, the kinetic energy and the total energy of the drops from figure 6 are plotted versus time. Initially, the kinetic energy is increased by the force that accelerates the drops together. Since this force is not constant (it increases linearly with distance from the center of the computational box) the increase is not quadratic as for the computations reported in Nobari, Jan, and Tryggvason[11]. After the force has been turned off, the drops move a short distance before colliding. Since the ambient fluid has a finite viscosity, kinetic energy is dissipated due to friction and the drops slow down. As the drops come in contact, the kinetic energy of the low impact number drops decreases rapidly, but the high impact number drops are not affected to any significant degree. Similarly, the surface tension energy of the low impact number drops increases and the drops deform, but the surface tension energy of the other drops hardly increases at all since the drops remain almost spherical. When the film between the drops is ruptured, part of the drops surface is removed and the surface energy reduced. This reduction is larger for the low impact number drops since the area removed is larger. Initially, the kinetic energy of

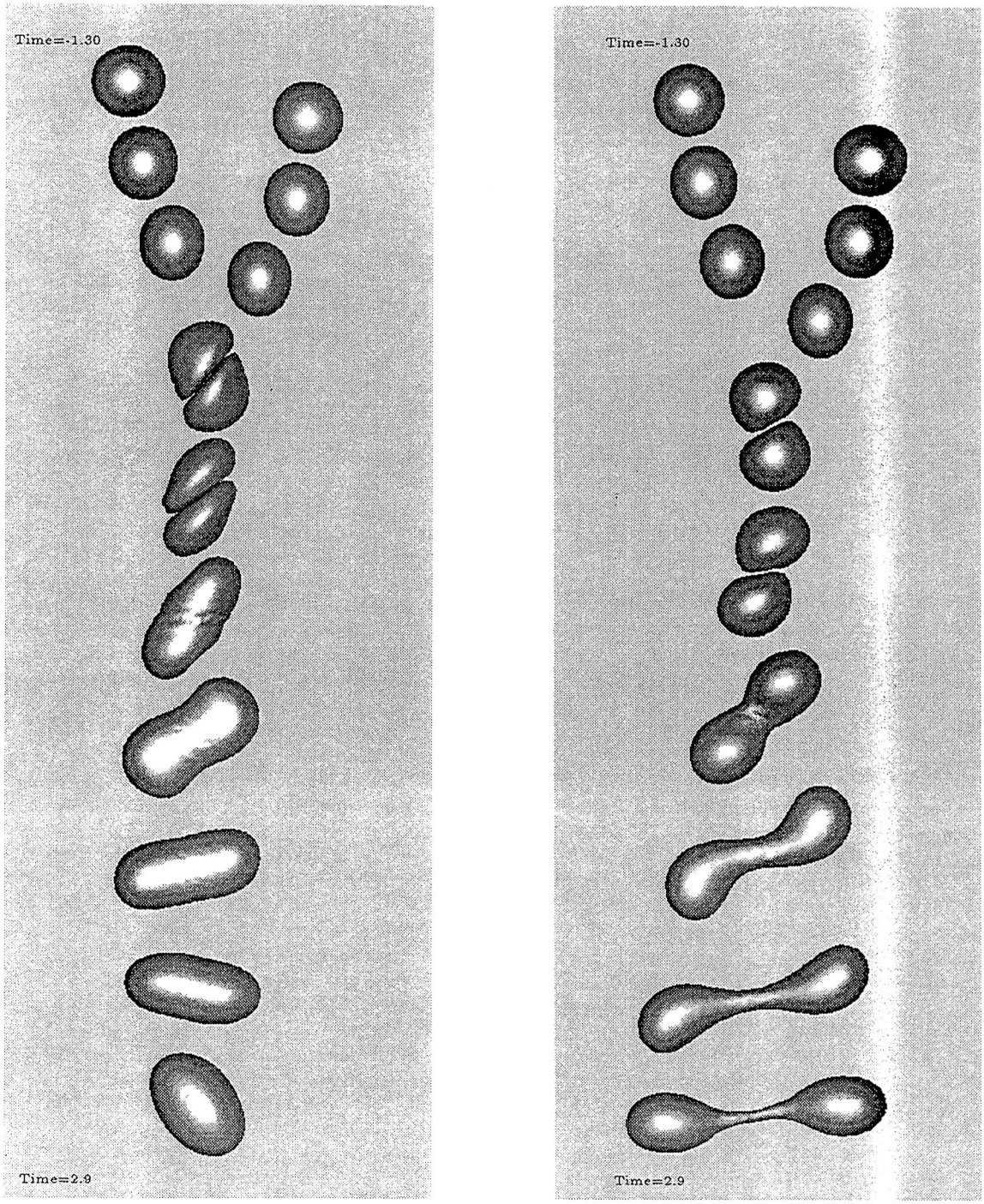

Figure 6. Coalescing collisions. The initial conditions are shown at the top of the figure and the pair is then shown every 0.42 time units. The film is ruptured at t=0.46 in both cases, but the impact parameter is different for the two runs. In the left column I=0.5, and I=0.825 in the right one. For the low impact parameter, the drops coalesce permanently, but for the higher impact parameter they separate again.

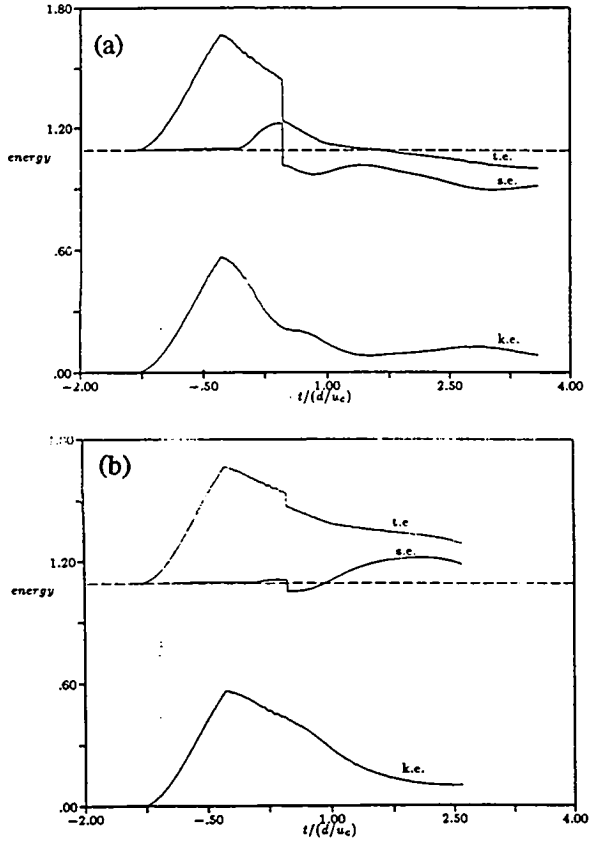

Figure 7. The energies for the drops in figure 6. (a) I=0.5, (b) I=0.825. The total energy, the surface energy and the kinetic energy of the drops are plotted versus time.

the high impact number drops is nearly unaffected (and continues to be dissipated at the same rate as before the drops collide), but as the coalesced drop starts to stretch and the surface tension energy to increase, the kinetic energy drops sharply. As the filament between the drops starts to neck down, the increase in surface area stops and the kinetic energy levels off. For the low impact number drops, the rupture takes place near the point of maximum deformation and surface energy is initially converted into kinetic energy as the drop adjusts to the new shape. The momentum of the drop before impact is, however, sufficiently large so the drop is stretched as the fluid of the original drops continue along the paths they were following before collision. This leads to an increase in surface tension energy and decrease in kinetic energy. When the surface tension energy reaches maximum the kinetic energy is not zero due to the finite rotational motion of the coalesced drop. Eventually, the coalesced drop oscillates.

For modeling of droplet collisions, the major question is whether the collision results in a single drop or not. Figure 8 shows our computations in the I-Re plane. In addition to the computations shown in figure 5, we have conducted two other calculations at different impact parameters. The runs that lead to a coalesced drops are shown by black squares and those leading to grazing collision as open squares. We have also plotted the experimental results of Jiang et al[3], for the boundary between these two collision modes for We=23. Their results do not extend down to the Reynolds number simulated here, but since the boundary is only weakly dependent on the Reynolds number it seems safe to extrapolate their results to our Reynolds number. The dashed line shows this extrapolation, showing that the numerical results are consistent with the experiments.

Conclusion

The purpose of this paper is to demonstrate the feasibility of accurate numerical predictions of fully three-dimensional off-axis collisions of two drops. To do so, we have simulated a few cases, both with and without rupturing of the interface separating the drops. Although the rupture of the film between the drops is done in an *ad hoc*, way, the results are in reasonably good agreement with experimental observations. For exact predictions of the boundary, a more accurate criteria for the rupture time[19] would have to be used. These computations, which require about ten hours on a CRAY-XMP, are done on a relatively coarse mesh and are therefore limited to relatively small Reynolds and Weber numbers. Nevertheless, they do demonstrate well the capability of the method.

Acknowledgment

We would like to acknowledge discussions with Dr. D. Jacqmin at the NASA Lewis Research Center. Part of this work was done while one of the authors (GT) was visiting the Institute for Computational Mechanics in Propulsion at NASA Lewis. This work is supported in part by NASA grant NAG3-1317, and NSF grant CTS-913214. Some of the computations were done at the San Diego Supercomputing Center which is funded by the National Science Foundation.

References

1. J. B. Heywood. Internal Combustion engine Fundamentals. McGraw-Hill, (1988). 930 pages.

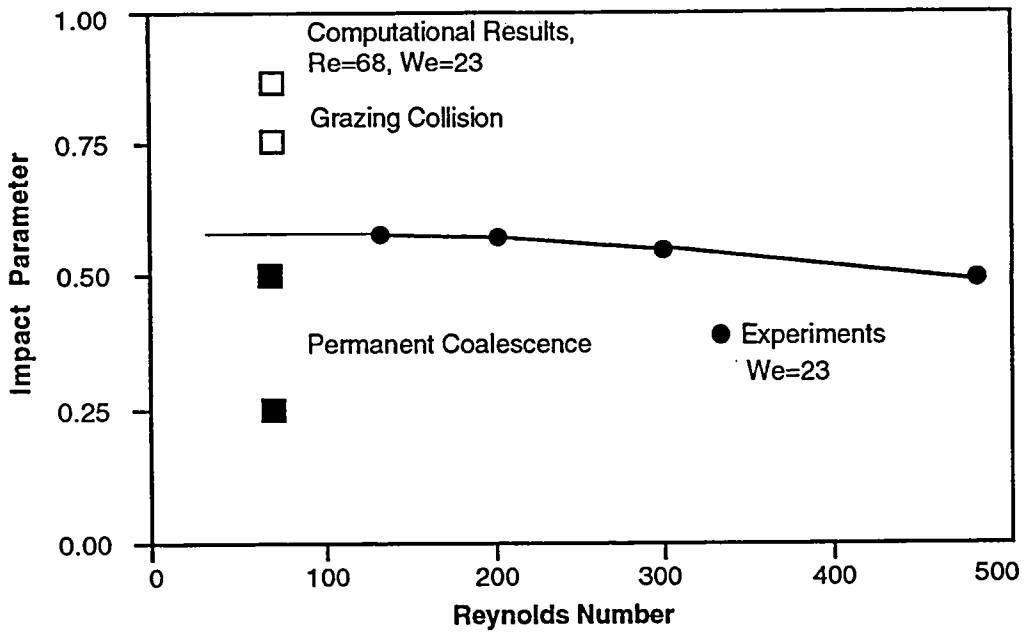

Figure 8. The boundaries between coalescing and grazing collisions in the Re-I plane for We=23. The solid circles, connected by a line, are experimental data from Jiang *et al*[3]. The squares are computed results.

2. N. Ashgriz and J.Y. Poo. Coalescence and separation in binary collisions of liquid drops. J. Fluid Mech. **221** (1990), 183-204.

3. Y.J. Jiang, A. Umemura, and C.K. Law. An experimental investigation on the collision behavior of hydrocarbon droplets. J. Fluid Mech. **234** (1992), 171-190.

4. S.G. Bradley and C.D. Stow. Collision between liquid drops. Phil. Trans. R.Soc. Lond. A **287** (1978), 635-678.

5. A.M. Podvysotsky and A.A. Shraiber. Coalescence and breakup of drops in two phase flows. Intl. J. Multiphase Flow **10** (1984), 195-209.

6. J.Y. Park and L.M. Blair. The effect of coalescence on drop size distribution in an agitated liquid-liquid dispersion. Chem. Engng. Sci. **30**, 1057-1064.

7. D.J. Ryley and B.N. Bennett-Cowell. The collision behavior of steam-borne water drops. Int. J. Mech. Sci. **9** (1967), 817-833.

8. P.R. Brazier-Smith, S.G. Jennings and J. Latham. The interaction of falling water drops: coalescence Proc. R. Soc. Lond. A **326** (1972), 393-408.

9. G.B. Foote. The Water Drop Rebound Problem: Dynamics of Collision. J. Atmos. Sci. **32** (1975), 390-402.

10. J. Fukai, Z. Zhao, D. Poulikakos, C.M. Megaridis, and O. Miyatake. Modeling of the deformation of a liquid droplet impinging upon a flat surface. Phys. Fluids A, **5** (1993), 2589-2599.

11. M.R.H. Nobari, Y.-J. Jan, and G. Tryggvason. Head-on collision of drops—A numerical investigation. Submitted for publication (1993).

12. S.O. Unverdi and G. Tryggvason. A Front Tracking Method for Viscous Incompressible Flows. J. Comput. Phys., **100** (1992) 25-37.

13. S.O. Unverdi and G. Tryggvason. Multifluid flows. Physica D **60** (1992) 70-83.

14. E.A. Ervin: *Full Numerical Simulations of Bubbles and Drops in Shear Flow*, Ph.D. Thesis, The University of Michigan, 1993.

15. A. Esmaeeli, E.A. Ervin, and G. Tryggvason: Numerical Simulations of Rising Bubbles. To appear in *Proceedings of the IUTAM Conference on Bubble Dynamics and Interfacial Phenomena* (Ed.: J.R. Blake)

16. Y.-J. Jan, and G. Tryggvason: Computational Studies of Contaminated Bubbles. Submitted for publication (1993).

17. M.R.H. Nobari and G. Tryggvason: Coalescence of Initially Stationary Drops. Submitted for publication (1993)

18. S. Nas and G. Tryggvason: Computational Investigation of the Thermal Migration of Bubbles and Drops. 1993 ASME Winter Annual Meeting.

19. D. Jacqmin and M.R. Foster. The evolution of thin films generated by the collision of highly deforming droplets. Submitted for publication (1993).

REPORT DOCUMENTATION PAGE

Form Approved
OMB No. 0704-0188

1. AGENCY USE ONLY (*Leave blank*)	2. REPORT DATE	3. REPORT TYPE AND DATES COVERED
	October 1994	Technical Memorandum

4. TITLE AND SUBTITLE

Numerical Simulations of Drop Collisions

5. FUNDING NUMBERS

WU-505-90-5K

6. AUTHOR(S)

M.R.H. Nobari and G. Tryggvason

7. PERFORMING ORGANIZATION NAME(S) AND ADDRESS(ES)

National Aeronautics and Space Administration
Lewis Research Center
Cleveland, Ohio 44135-3191

8. PERFORMING ORGANIZATION REPORT NUMBER

E-9167

9. SPONSORING/MONITORING AGENCY NAME(S) AND ADDRESS(ES)

National Aeronautics and Space Administration
Washington, D.C. 20546-0001

10. SPONSORING/MONITORING AGENCY REPORT NUMBER

NASA TM-106751
ICOMP-94-23
AIAA-94-0835

11. SUPPLEMENTARY NOTES

Prepared for the 32nd Aerospace Sciences Meeting and Exhibit sponsored by the American Institute for Aeronautics and Astronautics, Reno, Nevada, January 10-13, 1994. M.R.H. Nobari, University of Michigan, Ann Arbor, Michigan 48823; and G. Tryggvason, Institute for Computational Mechanics in Propulsion (work funded under NASA Cooperative Agreement NCC3-233), and University of Michigan, Ann Arbor, Michigan 48823. ICOMP Program Director, Louis A. Povinelli, organization code 2600, (216) 433-5818.

12a. DISTRIBUTION/AVAILABILITY STATEMENT

Unclassified - Unlimited
Subject Category 34

12b. DISTRIBUTION CODE

13. ABSTRACT (*Maximum 200 words*)

Three-dimensional simulations of the off-axis collisions of two drops are presented. The full Navier-Stokes equations are solved by a Front-Tracking/Finite-Difference method that allows a fully deformable fluid interface and the inclusion of surface tension. The drops are accelerated towards each other by a body force that is turned off before the drops collide. Depending on whether the interface between the drops is ruptured or not, the drops either bounce or coalesce. For drops that coalesce, the impact parameter, which measures how far the drops are off the symmetry line, determines the eventual outcome of the collision. For low impact parameters, the drops coalesce permanently, but for higher impact parameters, a grazing collision, where the drops coalesce and then stretch apart again is observed. The results are in agreement with experimental observations.

14. SUBJECT TERMS

Drop collisions; Front tracking

15. NUMBER OF PAGES

11

16. PRICE CODE

A03

17. SECURITY CLASSIFICATION OF REPORT	18. SECURITY CLASSIFICATION OF THIS PAGE	19. SECURITY CLASSIFICATION OF ABSTRACT	20. LIMITATION OF ABSTRACT
Unclassified	Unclassified	Unclassified	